JOURNAL OF MATERIALS SCIENCE 31 (1996) 4387–4394

Components of non-elastic deformation in amorphous glassy polymers

R. QUINSON*, J. PEREZ
Laboratoire GEMPPM, INSA, 69621 Villeurbanne Cedex, France
M. RINK, A. PAVAN
Dipartimento di Chimica Industriale e Ingegneria Chimica Giulio Natta, Politecnico di Milano, Piazza Leonardo da Vinci 32, 20133 Milano, Italy

Non-elastic deformation of amorphous polymers was studied from strain recovery tests. In particular, a strain recovery master curve was built, which allowed estimation of the recovery times necessary to recover the whole non-elastic deformation. On such a curve, two non-elastic deformations, one anelastic and one plastic, could be distinguished by their range of recovery time. The evolution of these two components was followed during a constant strain-rate test. This clearly showed the importance of the anelastic deformation. Finally, from a review of the properties of these two components, a consistent description of deformation and recovery processes has been proposed.

1. Introduction

When a polymer is deformed in the glassy state, three components of its deformation are commonly distinguished: elastic, anelastic and plastic deformation. To determine the value of each of these, the sample must be unloaded; the elastic strain recovers instantaneously, the anelastic one recovers in a lapse of time and the plastic one is permanent. However, several studies [1–4] have shown that the so-called plastic deformation can recover in a short time by bringing the polymer to or above the glass transition temperature, T_g. This total recovery also concerns the microstructural state, because the sample recovers its initial properties [5–7]. This recovery leads us to question the usual distinction of the two non-elastic deformations: anelastic and plastic. In a recent work, Nanzai [8] observed that in certain glassy polymers with a rigid structure such as polystyrene (PS), a real irreversible deformation can be observed. In any case, this deformation due to disentanglement remains very small and is only observed in PS. More generally, it is observed that amorphous glassy polymers subjected to large deformations (up to more than 50%) in the glassy state can recover their deformation at a temperature above T_g.

Aim of the present work was to investigate, at a macroscopic scale, the different components of non-elastic deformation by observing its recovery as a function of time and temperature in three amorphous polymers: polymethylmethacrylate (PMMA), polystyrene (PS) and polycarbonate (PC).

2. Experimental procedure

Materials, PMMA, PS, PC, were provided by Elf-Atochem. Differential scanning calorimetry (DSC) and gas-permeation chromatography (GPC) experiments were performed to determine the glass transition, T_g, and the average number molecular weight, M_n, of these materials: PMMA ($T_g = 120\,°C$, $M_n = 3000\,000$), PS ($T_g = 98\,°C$, $M_n = 124\,700$), PC ($T_g = 152\,°C$, $M_n = 23\,300$). Before being tested, all samples were brought to $T > T_g$ and then annealed at $T < T_g$. Such a treatment was performed in order to eliminate chain orientation and to confer a precise thermal history to the materials.

Two mechanical tests were carried out: uniaxial compression and plane strain compression. The uniaxial compression was performed on cylinders with dimensions ($L = 22$ mm, diameter $= 8$ mm) which permit buckling effects to be avoided and the barrelling effect to be minimized [9]. For the plane strain compression described elsewhere [10], the die breath was 3.5 mm and specimen width and thickness were 24 and 2 mm, respectively. These dimensions meet conditions to have the best plane strain state [10, 11]. In addition, friction between dies and sample becomes negligible with the application of a PTFE spray (Lubriflon).

During loading and after unloading, the strain is measured by means of an extensometer fixed on the sample in the case of uniaxial compression. In the plane strain compression test, the strain at the loading stage is measured by means of a very accurate strain gauge system fixed on the dies. The residual strain after unloading is obtained by measuring the difference between the deformed and the undeformed part of the sample with an LVDT transducer. These devices have been developed and used in previous studies [12–14].

Both tests were carried out on an Instron 1185 equipped with a 100 kN cell. During loading, strain

* Author to whom all correspondence should be addressed.

0022–2461

rate was 0.1 min^{-1} which leads to an average loading time of 2 min. The unloading rate was ten times faster than the loading one.

Strain, ε, and stress, σ, are derived from measurements via

$$\varepsilon = \frac{l_0 - l}{l}$$

$$\sigma = \frac{F}{S_0(1 - \nu\varepsilon)^2}$$

in uniaxial compression, and

$$\sigma = \frac{F}{S_0}$$

in plane strain compression (the stressed section under the dies remains constant), where l is the sample length, l_0, S_0 the initial length and initial section of the sample, F the applied force, and ν is Poisson's ratio taken as 0.5 (constant volume).

3. Strain recovery experiments

3.1. Recovery as a function of time

Under fixed experimental conditions, several samples were deformed up to different strain levels, and then unloaded and measured after a given recovery time. So, we can determine the residual strain, ε_{res}, after a given recovery time, t_{rec}, for different applied strain levels, ε_t. The stress and the residual strain are reported as a function of the applied strain on a double ordinate plot (Fig. 1). The residual strain is reported for different recovery times. Obviously, for a given applied strain, the residual strain decreases as the recovery time increases. In addition, the strain recovery kinetics depends on recovery temperature, T_{rec}. Indeed, for T_{rec} well below T_g, the kinetics is slow, whereas for T_{rec} close to T_g, it becomes faster. The slow strain recovery kinetics for PC at 20 °C (Fig. 1) and the fast one for PS at 90 °C which features a quasi-total recovery after 200 h (Fig. 2), illustrate this comment. Last but not least, these curves show that the value of the applied strain that corresponds to the residual deformation onset (yield strain) is independent of the recovery time in the studied time range. We observe that the associated stress (yield stress) cannot be identified with the maximum of the stress–strain curve. This last observation is in accordance with previous ones on PC [12–14] and on linear polyethylene [15]. Such a yield-stress determination for different stress states has also allowed the validity of yield criteria to be checked accurately [12–14].

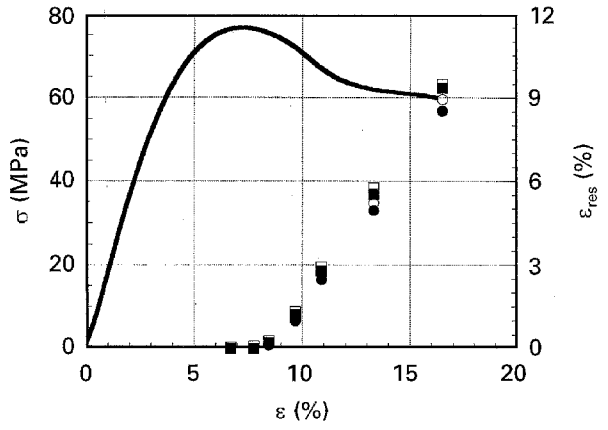

Figure 1 Dependence of residual strain, ε_{res}, on recovery time, t_{rec}, at a temperature $T_{rec} = T_{def}$ far below T_g. PC, uniaxial compression, $d\varepsilon/dt = 2 \times 10^{-3}\ s^{-1}$, $T_{def} = 20\,°C$: $\sigma = f(\varepsilon)$; $\varepsilon_{res} = f(\varepsilon_t)$ at $T_{rec} = 20\,°C$ for recovery times, $t_{rec} =$ (□) 10 min, (■) 60 min, (○) 3600 min, (●) 50 000 min.

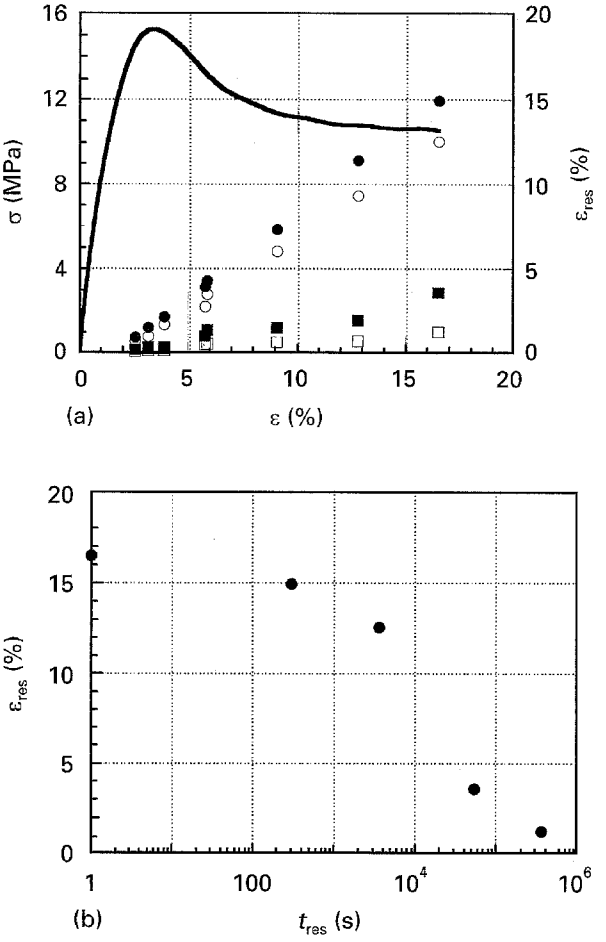

Figure 2 Dependence of residual strain, ε_{res}, on recovery time, t_{rec}, at a temperature $T_{rec} = T_{def}$ close to T_g. PC, uniaxial compression, $d\varepsilon/dt = 2 \times 10^{-3}\ s^{-1}$, $T_{def} = 90\,°C$. (a) As in Fig. 1, $\varepsilon_{res} = f(\varepsilon_t)$ at $T_{rec} = 90\,°C$ for recovery times, $t_{rec} =$ (●) 5 min, (○) 60 min, (■) 900 min, (□) 6000 min; (b) $\varepsilon_{res} = f(t_{rec})$ for $\varepsilon_t = 16.5\%$.

3.2. Recovery as a function of temperature

The temperature effect on strain recovery was investigated by deforming a specimen at a fixed temperature and by measuring the residual strain after a given recovery time at different temperatures. Fig. 3 features the stress/strain curve of PMMA deformed in plane strain compression at 20 °C and the residual strains measured after 15 h at different recovery temperatures. The recovery is quite regular up to 100 °C after which it accelerates and becomes very large. After 15 h at 120 °C, the deformation disappears fully whatever the applied strain. Similar results were observed on PMMA deformed in uniaxial compression at − 100 °C [16].

From these results, we can distinguish two modes of strain recovery. The first one corresponds to a slow

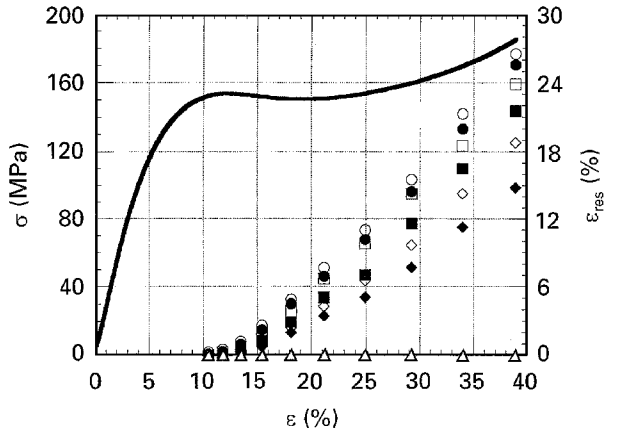

Figure 3 Dependence of residual strain, ε_{res}, on recovery temperature, T_{rec}, at a given recovery time, t_{rec}. PMMA, plane strain compression, $d\varepsilon/dt = 2 \times 10^{-3}\ s^{-1}$, $T_{def} = 20\,°C$. As in Fig. 1, $\varepsilon_{res} = f(\varepsilon_t)$ at $t_{rec} = 15$ h for T_{rec} = (○) 20, (●) 40, (□) 60, (■) 80, (◇) 100, (◆) 110, (△) 120 °C.

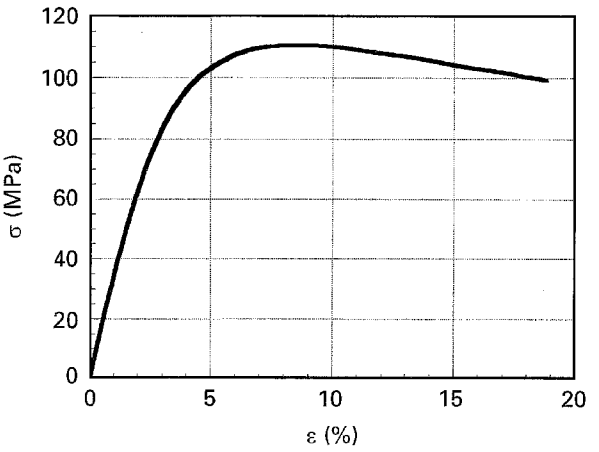

Figure 4 $\sigma = f(\varepsilon)$ for PMMA, uniaxial compression, $\varepsilon = 2 \times 10^{-3}\ s^{-1}$, $T_{def} = 20\,°C$, $\varepsilon_t = 19\%$.

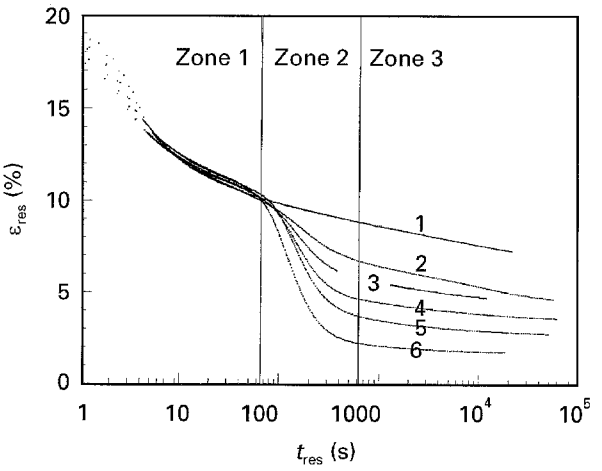

Figure 5 Strain recovery kinetics for several T_{rec} in PMMA deformed up to 19% under the same conditions as in Fig. 4. Zone 1, before putting the sample in the oven. Zone 2, before temperature stabilization in the sample. Zone 3, at constant recovery temperature, T_{rec} = (1) 20 °C, (2) 40 °C, (3) 50 °C, (4) 60 °C, (5) 70 °C, (6) 90 °C.

and regular recovery, and is observed up to a temperature lower than approximately $T_g - 20\,°C$. The second one is very fast and is observed at temperatures near T_g.

3.3. Strain recovery master curve

From these results the thermal activation effect on recovery processes stands out beyond doubt. Accordingly, it may be possible to build a strain recovery master curve by applying a time–temperature reduction scheme such as those used for viscoelastic properties, using the time–temperature equivalence principle [17]. The strain recovery master curve was built from isothermal recovery curves obtained at different temperatures after loading a test sample up to a fixed deformation. The isotherms were then shifted along the log time axis, in order to obtain best superposition.

Two experimental procedures were used to obtain the isothermal recovery curves of PMMA samples strained up to 19% in uniaxial compression at 20 °C (Fig. 4). The first one consisted in following the strain recovery for 15 h at several temperatures using a different sample for each recovery temperature (Fig. 5). In the second one, the same strained sample was used to measure a 1 h recovery segment for each temperature, the temperature being increased in steps. In both cases, the $\varepsilon = f(\log t)$ recovery segments obtained were corrected before their use in the master curve construction as follows. First, the recovery time origin for each segment was set at the time when the recovery temperature was reached: with our samples, this time was about 10 min. Second, sample thermal dilatation between the reference temperature (20 °C) and the recovery temperature must be taken into account. This was done by shifting the $\varepsilon = f(\log t)$ recovery segments vertically by an amount equivalent to the dilatation calculated using a value of $8\ 10^{-5}\ K^{-1}$ for the dilatation coefficient of PMMA in the used temperature range. A third correction ought to be applied to the second procedure used. For each temperature, the recovery times of the preceding temperatures steps are equivalent to some recovery time at this temperature, and this time ought to be added to the origin of the new segment. In all cases, this time (estimated from shift factors) was lower than 5 min and was neglected.

The two strain recovery master curves produced by shifting the relevant strain recovery segments obtained according to the two procedures described above are shown in Fig. 6 together with the relative shift factors (inset). It is comforting to observe that both procedures lead to similar master curves and similar shift factors. The right-hand side of the master curve comes from the recovery segment at 115 °C. Such an acceleration of strain recovery has already been observed for PS at 90 °C (Fig. 2b).

In spite of the similarity of the two master curves obtained, they must be considered cautiously. Indeed, a slight error in the recovery segment shape obtained after treatment can lead to an incorrect shift which reflects in the shape of the master curve. Therefore, the time values extracted from this master curve may not

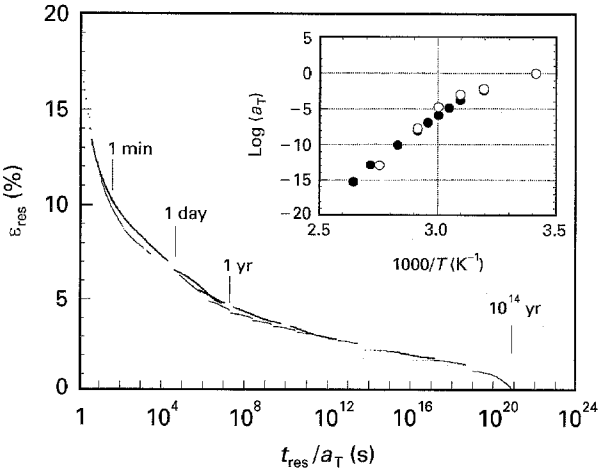

Figure 6 Strain recovery master curve at $T_{rec} = 20\,°C$ for PMMA deformed under the same conditions as in Fig. 4: master curves obtained following two different experimental procedures (see text) and corresponding shift factors: (○) procedure 1, (●) procedure 2.

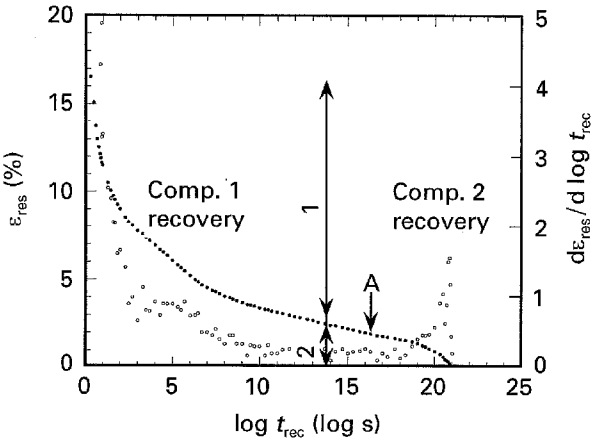

Figure 7 PMMA strain recovery curve at $T_{rec} = 20\,°C$ (from Fig. 6) and its derivative. Two well-distinguished zones corresponding to component 1 which recovers at short t_{rec} and component 2 which recovers at very long t_{rec}. Point A indicates the calculated time at 20 °C corresponding to 1 h at 100 °C ($T_g - 20\,°C$).

be very accurate. However, the whole aspect of this curve should not be questioned.

4. Discussion

4.1. Two strain recovery stages

By deriving the master curve (Fig. 7), one can estimate the characteristic strain recovery time distribution of the whole non-elastic deformation. In spite of the reservation expressed above, we can comment, at least qualitatively, on the shape of this distribution. Thus, this curve confirms the presence of two non-elastic strain components exhibiting distinct recovery time distributions.

The first component (component 1) presents a distribution covering at least ten decades of time: at 20 °C it extends from the very beginning of the recovery experiment to times of about 10^{10} s. We note that the unloading time employed (a few seconds) prevented us from following the recovery kinetics at times shorter than 10 s. Consequently, the derivative curve obtained only features a part of this characteristic time distribution. Using an Arrhenius treatment, the shift factors of Fig. 6 provide information on apparent activation energy for the recovery processes associated with component 1. We can observe an increase in apparent activation energy with recovery temperature (or recovery time) from about 220 kJ mol^{-1} to about 650 kJ mol^{-1}.

The second component (component 2) presents a distribution covering about two decades of time: at 20 °C the recovery times are of the order of about one billion years. It is impossible to estimate the apparent activation energy of this component from these experiments. Indeed, all the associated deformation abruptly recovers during the single isothermal segment at 115 °C.

As expected, recovery may be observed in shorter times by increasing the temperature. In fact, component 2 is completely recovered in a few hours for PS at 90 °C, and in a few minutes for PMMA at 115 °C. It should be noted that these temperatures are close to T_g of the polymer: $T_g - 8\,°C$ for PS and $T_g - 5\,°C$ for PMMA.

It can be observed from Fig. 7 that in the case of PMMA strained up to 19% in uniaxial compression at 20 °C (Fig. 4), components 1 and 2 amount to about 14% and 2.5%, respectively (the other 2.5% being purely elastic). It is worth noting that beyond the maximum stress ($\varepsilon = 8\%$), only a minor part of the additional 11% strain can be attributed to component 2. Accordingly, component 1 continues to grow beyond this maximum.

Several authors [18–20] have measured the non-elastic strain recovery while scanning the temperature by a linear increase. They found $\varepsilon_{res} = f(T_{rec})$ and $d\varepsilon_{res}/dT_{rec} = f(T_{rec})$ curves similar to $\varepsilon_{res} = f(\log t_{rec})$ and $d\varepsilon_{res}/d \log t_{rec} = f(\log t_{rec})$ curves presented here (Fig. 7) which is not surprising in view of the time–temperature equivalence. However, because their technique prevents them from observing the fastest recovery processes occurring during unloading, the low-temperature peak they observed is likely to be an artefact. In agreement with our results on PMMA, Oleynik and co-workers [5, 18, 21, 22] have shown the existence of two distinct components during strain recovery of several polymers strained at temperatures far below T_g. Owing to the fact that component 2 recovers only after very long times, whereas component 1 is mostly recovered after the usual observation times, the two can be conventionally called plastic (ε_{pl}) and anelastic (ε_{an}) deformation, respectively. However, at T near T_g, the recovery times relative to component 2 (ε_{pl}) also become very short and the two components are no longer distinguishable (Fig. 2b).

4.2. Anelastic and plastic strain variation during a mechanical test

From our results and those of Oleynik, it appears that a treatment of about 1 h at $T_g - 20\,°C$ on a sample strained at T_{def} far below T_g, allows the total recovery of ε_{an} while ε_{pl} remains in the sample. Indeed, from the

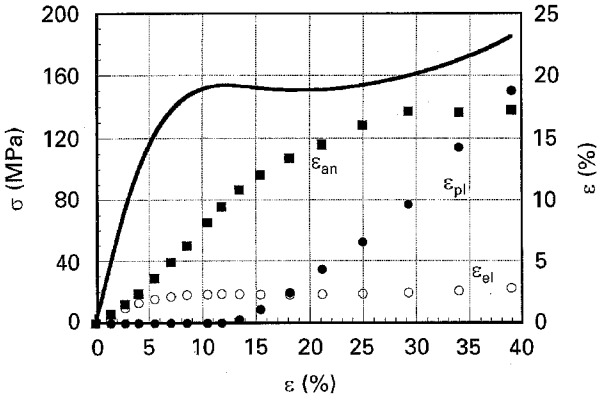

Figure 8 Variation of (○) ε_{el}, (■) ε_{an} and (●) ε_{pl} during deformation in PMMA in plane strain compression, PMMA, $d\varepsilon/dt = 2 \times 10^{-3}\,s^{-1}$, $T_{def} = 20\,°C$.

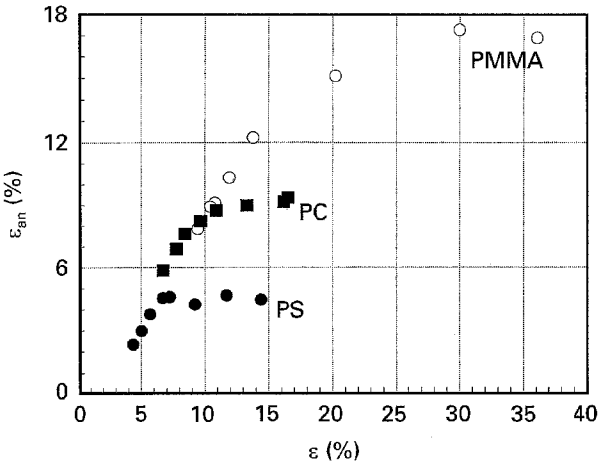

Figure 9 Comparison of $\varepsilon_{an} = f(\varepsilon_t)$ in three polymers (●) PS, (■) PC, (○) PMMA, under uniaxial compression, $d\varepsilon/dt = 2 \times 10^{-3}\,s^{-1}$, $T_{def} = 20\,°C$.

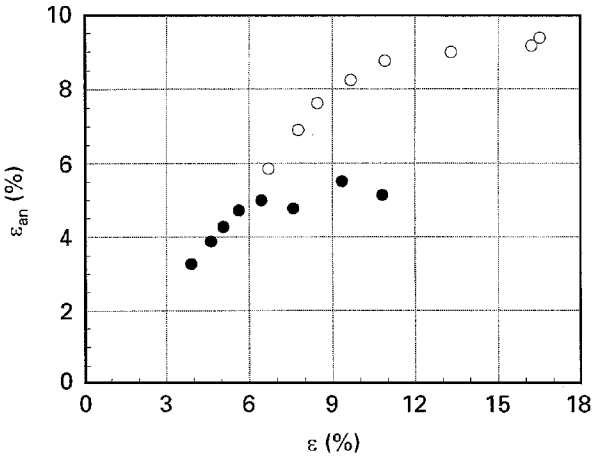

Figure 10 Comparison of $\varepsilon_{an} = f(\varepsilon_t)$ at two different temperatures, T_{def} (○) 20 °C and (●) 90 °C, in PC, uniaxial compression, $d\varepsilon/dt = 2 \times 10^{-3}\,s^{-1}$.

shift factors reported in Fig. 6 it is possible to estimate the time at 20 °C equivalent to 1 h at $T_g - 20\,°C$. That time is indicated by an arrow (A) in Fig. 7. It clearly falls before the plastic strain recovery times. Thus, by applying the treatment of 1 h at $T_g - 20\,°C$, and because $\varepsilon_{res} = \varepsilon_{pl}$ after that treatment, we can determine ε_{pl} as a function of the total deformation applied before unloading, ε_t. Then we can determine the value reached by ε_{an} before unloading as $\varepsilon_{an} = \varepsilon_t - \varepsilon_{el} - \varepsilon_{pl}$, in which ε_{el}, the purely elastic deformation, is calculated from $\varepsilon_{el} = E_{ur}\sigma_t$, with E_{ur}, the unrelaxed modulus measured at very high frequency or at very low temperature and σ_t the stress value just before unloading.

From Fig. 8, which shows ε_{el}, ε_{an} and ε_{pl} variation with the applied strain for PMMA strained at 20 °C in plane strain compression (E_{ur} taken from [23]), it can be observed that ε_{an} onsets from the very beginning of the test and keeps growing even beyond the maximum stress. It levels off when the stress reaches its minimum value. In addition, ε_{pl} onsets around the maximum stress and then increases continuously as the strain increases. It must be emphasized that the stress peak develops when ε_{an}, is increasing greatly while ε_{pl} is just setting in. Then, the strain rate around this peak is mainly due to ε_{an}. On a PS notched sample, a similar result was deduced from optical observations [24].

A constant ε_{pl} rate is only reached in the minimum stress zone when ε_{an} becomes constant. Consequently, this zone corresponds to a stationary regime of deformation, as has already been observed [8, 25, 26]. Activation volume and activation energy associated with ε_{pl} ought to be calculated in this state.

4.3. Properties and the nature of non-elastic strain components

From our results and those reported by other authors, it is possible to draw up a list of properties associated to the two non-elastic strain components.

4.3.1. Anelastic deformation

Anelastic deformation depends on the polymer (Fig. 9), and also on temperature, diminishing as T_{def} increases, at least over the temperature range here examined, i.e. 20–90 °C (see, for example, Fig. 10) and it is expected to become negligible when $T_{def} > T_g$ [5].

ε_{an} is necessary to create ε_{pl}. Indeed, Oleynik [5] shows that a prestrained sample heated to some $T < T_g$ to eliminate ε_{an} but still featuring ε_{pl}, when deformed a second time, requires a certain amount of ε_{an} before creating further ε_{pl}.

ε_{an} has been associated with a slight material densification (volume decrease), at least in compression [27].

From mechanical spectrometry tests below T_g [28, 29], a strained sample is found to feature a larger molecular mobility than an unstrained one. This extra mobility can be associated with ε_{an} because a treatment erasing ε_{an} also erases this excess mobility.

During sample deformation, a large amount of energy, ΔU, is stored in the sample and has been measured [5, 22, 30, 31]. This energy increases from the very beginning of the deformation and levels off at a value of about 14 $J\,g^{-1}$ for PMMA, 10 $J\,g^{-1}$ for PS and 8 $J\,g^{-1}$ for PC [32] at deformations well above the maximum stress deformation. Up to large applied

deformations (about 30%), this stored energy is released if the sample is heated to $T < T_g$ (DSC experiments) [22, 33, 34] thus showing its association with ε_{an}. Also, the similar aspect of the evolution of ΔU [32] and ε_{an} (Fig. 9) with both quantities levelling off, points to a direct link between ΔU and ε_{an}.

Fig. 11a shows that the relationship between applied stress and ε_{an} depends on the initial microstructural state.

Apparent activation energies deduced from our shift factors (Fig. 6) are very similar to those obtained for the α relaxation peak in mechanical spectrometry [35]. In this latter case, the apparent activation energy is about 280 kJ mol^{-1} for the low-temperature part of the α peak which corresponds to an isostructural state. Then, it increases with temperature up to more than 550 kJ mol^{-1} owing to the evolution of the microstructural state of the material. These values are very closed to ours (220–650 kJ mol^{-1}). This leads us to think that the recovery processes of ε_{an} (component 1 in our master curve) and processes probed in mechanical spectrometry in the low-temperature part of the α relaxation peak, are similar. This result is confirmed by another result [32] which shows, from thermostimulated creep tests, that activation energies of recovery processes are close to those which are associated with molecular motions observed between T_{def} and T_g. Moreover, these apparent activation energies are independent of T_{def} and ε_t [32]. In other terms, these results clearly show that all motions probed in mechanical spectrometry in the linear regime (very low stress) up to about the α peak maximum are activated under the high stress (non-linear regime) during a constant strain-rate test at temperatures much lower than T_α. This observation agrees with the finding of a previous study [36] showing that the α peak is shifted towards lower temperatures as the applied stress is increased.

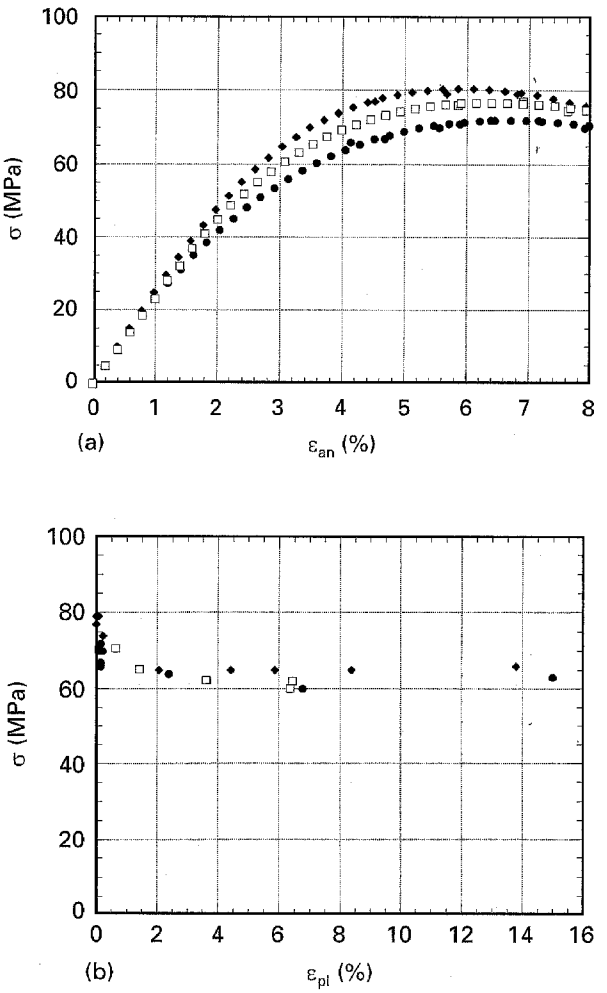

Figure 11 (a) $\sigma = f(\varepsilon_{an})$ and (b) $\sigma = f(\varepsilon_{pl})$ for different initial microstructural states. PC, uniaxial compression, $d\varepsilon/dt = 2 \times 10^{-3}$ s^{-1}, $T_{def} = 20$ °C. Three initial states obtained after different cooling rate from $T > T_g$: (◆) 0.02 °C min^{-1}, (□) 1 °C min^{-1}, (●) quenching in water and ice.

4.3.2. Plastic deformation

For large applied deformations, this component is always present whatever the test temperature ($T_{def} < T_g$ or $T_{def} > T_g$) and always recovers in the T_g zone during heating of the sample [5].

It corresponds to a large conformational change (*gauche–trans*) [5] leading to chain orientation, but no volume change seems to be associated with ε_{pl} [27].

Heat release due to this component recovery as measured in a DSC, is only observed at high strains and remains smaller than that corresponding to ε_{an} [33, 34].

Fig. 11b shows that, unlike ε_{an}, the relation between ε_{pl} and σ is independent of the initial microstructural state of the material (except for low values of ε_{pl} where ε_{an} keeps growing).

On PS [37], the study of ε_{pl} recovery kinetics shows that the associated apparent activation energy diminishes as recovery temperature increases. It decreases from 260 kJ mol^{-1} to 130 kJ mol^{-1} as T_{rec} increases near T_g. Moreover, Andrews [38] has shown that these apparent activation energies are independent of ε_t. It is important to observe that in this temperature range, the apparent activation energy of the α relaxation ensued from the master curve of the PS obtained with mechanical spectrometry [39] decreases as the temperature increases from 200 kJ mol^{-1} to 130 kJ mol^{-1}. Thus, these values, which correspond to the high-temperature part of the α relaxation, feature the same evolution and the same values as those corresponding to recovery processes of ε_{pl}. This result leads us to think that processes corresponding to ε_{pl} and to the high-temperature part of the α relaxation peak, have the same nature.

4.4. Description of molecular processes

The features of the deformation components observed experimentally lead to specific descriptions of the deformation processes in the glassy state previously proposed by Perez *et al.* [26, 40–42].

4.4.1. Anelastic deformation processes

Under an applied stress, deformation occurs in relation with pre-existing defects, called quasi-point defects [43]. Defect concentration is affected by thermal treatment (structural relaxation); it decreases when the sample is well

annealed [44]. This concept of deformation localization in pre-existing defects is also assumed by other authors [45].

These localized strained zones are called shear micro-domains (SMD). After unloading, these unstable zones recover due to elastic line energy at the borders of the SMD in the undeformed matrix. This recovery process was first proposed by Bowden and Raha [46]. These SMD are then at the origin of ε_{an}. The zones remain local and do not lead to chain orientation as no important change in the population of *gauche* or *trans* conformations are experimentally observed [5, 47]. Moreover, SMD growth occurs mainly by shearing because (i) it is associated with a very slight volume variation [27], and (ii) hydrostatic pressure by itself does not create the stored energy associated with ε_{an} [32]. Nevertheless, no experimental data are categorical about the real nature of molecular motions leading to SMD growth. Anyway, as we have seen, the nature of these motions is similar to that of the motions probed in mechanical spectrometry in the anelastic part of the α relaxation [32, 36]. Kung and Li [27] describe these motions as localized conformational changes (which must be different from *gauche* or *trans* conformations); in his self-consistent model, Perez [43] describes them as a correlation of elementary motions (β motions) corresponding to conformational changes.

According to such a description, the stored energy associated with ε_{an} is mainly due to the expansion of the SMD in an undeformed matrix by a new defect generation or molecular diffusion [26]. In the case of well-annealed samples (Fig. 11a), the extra mechanical energy, supplied to create ε_{an}, is due to the difficulty of creating larger SMD as there are fewer initial defects.

4.4.2. Plastic deformation processes

When the SMD are numerous enough or large enough to interact with one another, they can annihilate their line energy. This SMD interaction and annihilation corresponds to the creation of a large local perturbation permitting a large motion of macromolecular chains leading to some conformational orientation. Therefore, the work of deformation associated with ε_{pl}, leading to a heat release measured in the DSC during ε_{pl} recovery, corresponds mainly to a change in entropy. When the SMD are annihilated to give plastic zones, other SMD are created at plastic zone borders where disturbed zones or defects subsist. Thus, plastic zones ought to be always surrounded with anelastic zones.

It is worthwhile noting that such a description is consistent with experimental observation of shear bands on PS [3, 24, 48]. When the stress is applied, diffuse shear zones [24] made of "fine slip bands" [3], are first created and are mainly anelastic [24, 48], corresponding then to ε_{an}. Then, from these zones, shear bands containing large deformations appear. These bands only recover near T_g for the usual time scale [1, 4] and then, can be associated with ε_{pl}. Under stress, diffuse zones always surround these shear bands. Moreover, microscopic observations after different types of creep/recovery tests [48] clearly show that the shear band expansion needs a certain amount of ε_{an}.

4.4.3. Stationary regime

During deformation, new defects are mainly generated by anelastic deformation, i.e. because of SMD expansion. Their nature appears to be similar to pre-existing defects as the enthalpy relaxation kinetics associated with their relaxation appears to be the same but shifted to smaller time [49]. There is then a competition between defects creation due to anelastic deformation and defects annihilation due to structural relaxation. This competition leads to a defect population equilibrium, independent of the initial microstructural state corresponding to the stationary regime [26].

4.4.4. Strain recovery processes

Confirming other results [27, 50], we have clearly shown that the non-elastic strain recovery is a two-stage process. Each stage corresponds to one non-elastic deformation component.

After unloading, most of the SMD (ε_{an}) quickly recover at the loading temperature due to the surrounded undeformed matrix [36]. The more stable ones require a larger thermal energy to recover. However, they always recover at a temperature well below T_g. In addition, this strain recovery is accompanied by the associated energy release.

Plastic deformation corresponds to chain orientation and leads to the appearance of a rubber-like entropic force [25, 51] which tends to recover this deformation. However, new configurations due to chain orientation are rather stable and intermolecular forces at $T < T_g$ prevent macromolecular chains from coming back to their initial state. Consequently, for the usual times, it is necessary to go up to T_g to make intermolecular forces weaker and to permit oriented chains, subjected to an entropic force, to return to their unoriented state.

5. Conclusion

From different strain recovery tests and from a strain recovery master curve, two distinct components of the non elastic deformation are clearly identified when temperature is lower than about $T_g - 30\,°C$: (i) an anelastic component, ε_{an}, which recovers over a large range of time (at least ten decades) spanning from very short times to some 10^{10} s in PMMA at 20 °C, and (ii) a plastic component, ε_{pl}, which recovers over a range of time of about two decades, which is located around one billion years for PMMA at 20 °C. This component can recover in a few hours by bringing the polymer close to its T_g.

On a classic stress–strain curve, the maximum stress is observed to occur while a large increase of anelastic deformation is still taking place. The strain increase is mainly anelastic at this maximum and becomes fully

plastic around the minimum stress corresponding to the beginning of the stationary regime.

Through our experimental results and those of other authors, a description of deformation processes previously proposed by Perez *et al.* [26, 40, 42] can be specified. At a microscopic level, the anelastic deformation is associated with localized SMD. These SMD correspond to an increase in potential energy. After unloading, most of these SMD quickly recover at T_{def}. The plastic deformation results from SMD interaction and annihilation and corresponds to a chain orientation which creates a rubber-like entropic force. Chain orientation corresponds to new stable configurations and requires a very long time or a high thermal energy (temperature close to T_g) to return to the initial configuration under the effect of the entropic force.

This study emphasizes the importance of the anelastic deformation. Indeed, it appears that this deformation must not be neglected to understand and model the plastic behaviour of polymers.

The proposed description is consistent with experimental observation but still remains qualitative. A modification of a previous model [26] is now under study to describe the strain recovery and, more generally, all the macroscopic observations related to anelastic and plastic deformation.

Acknowledgement

This study, carried out in laboratories of Politecnico di Milano, was supported by Elf Atochem.

References

1. A. S. ARGON, R. D. ANDREWS, J. A. GODRICK and W. WITHNEY, *J. Appl. Phys.* **39** (1968) 1899.
2. W. WU and P. L. TURNER, *J. Polym. Sci. Polym. Phys.* **11** (1973) 2199.
3. J. B. C. WU and J. C. M. LI, *J. Mater. Sci.* **11** (1976) 434.
4. J. C. M. LI, *Met. Trans.* **9A** (1978) 1353.
5. E. OLEYNIK, *Prog. Colloid Polym. Sci.* **80** (1989) 140.
6. O. A. HASSAN, M. C. BOYCE, X. S. LI and S. BERKO, *J. Polym. Sci. Polym. Phys.* **31** (1993) 185.
7. C. C. CHAU and J. C. M. LI, *J. Mater. Sci.* **17** (1982) 652.
8. Y. NANZAI, *Prog. Polym. Sci.* **18** (1993) 437.
9. C.G'SELL, in "Plastic deformation of amorphous and semi-crystalline materials" eds B. Escaig and C. G'self (les Éditions Physiques Les Ullis, 1982) p. 13.
10. J. G. WILLIAMS and H. FORD, *J. Mech. Eng. Sci.* **6** (1964) 405.
11. A. P. GREEN, *Philos. Mag.* **42** (1951) 900.
12. R. BIANCHI and A. TESTI, thesis, Politecnico di Milano (1991).
13. R. QUINSON, PhD thesis, INSA Lyon (1995).
14. R. QUINSON, J. PEREZ, M. RINK and A. PAVAN, *J. Mater. Sci.* forthcoming.
15. D. G. FOTHERINGHAM and B. W. CHERRY, *J. Mater. Sci.* **13** (1978) 231.
16. A. S. ARGON and M. I. BESSONOV, *Polym. Eng. Sci.* **17** (1977) 174.
17. J. D. FERRY, "Viscoelastic properties of polymers" (Wiley, New York, 1980).
18. E. OLEYNIK, *Polym. J.* **19** (1987) 105.
19. T. KATO, *J. Appl. Polym. Sci.* **22** (1989) 1767.
20. G. W. ADAMS and R. J. FARRIS, *Polymer* **60** (1989) 1829.
21. S. S. SHEIKO, O. B. SALAMANTINA, S. N. RUDNEV and E. F. OLEYNIK, *Polym. Sci.* USSR **32** (1990) 1759.
22. E. OLEYNIK, in "High performance polymers" edited by E. Baer and S. Moet, Hanser Verlag, Munscher (1990) 60.
23. A. F. YEE and M. T. TAKEMORI, *J. Polym. Sci. Polym. Phys.* **20** (1982) 205.
24. E. J. KRAMER, *J. Macromol. Sci. Phys.* **B10** (1974) 191.
25. C. G'SELL and J. J. JONAS, *J. Mater. Sci.* **16** (1981) 1956.
26. M. B. M. MANGION, J. Y. CAVAILLE and J. PEREZ, *Philos. Mag. A* **66** (1992) 773.
27. T. M. KUNG and J. C. M. LI, *J. Mater. Sci.* **22** (1987) 3620.
28. L. DAVID and S. ETIENNE, *Macromolecules* **25** (1992) 4302.
29. C. G'SELL, H. EL BAHRI, J. PEREZ, J. Y. CAVAILLE and G. P. JOHARI, *Mater. Sci. Eng.* **A110** (1989) 223.
30. S. N. RUDNEV, O. B. SALAMANTINA, V. V. VOENNIY and E. F. OLEYNIK, *Coll. Polym. Sci.* **269** (1991) 460.
31. G. W. ADAMS and R. J. FARRIS, *Polymer* **60** (1989) 1825.
32. E. F. OLEYNIK, O. B. SALAMANTINA, S. N. RUDNEV and S. V. SHENOGIN, *Polym. Sci.* USSR **35** (1993) 1532.
33. O. A. HASSAN and M. C. BOYCE, *Polymer* **34** (1993) 5085.
34. B. T. CHANG and J. C. M. LI, *Polym. Eng. Sci.* **28** (1988) 1198.
35. E. MUZEAU, PhD thesis, INSA Lyon (1992).
36. R. QUINSON, J. PEREZ, Y. GERMAIN and J. M. MURRACIOLE, *Polymer*, **36** (1995) 743.
37. B. T. A. CHANG and J. C. M. LI, *J. Mater. Sci.* **16** (1981) 889.
38. R. D. ANDREWS, *J. Appl. Phys.* **26** (1955) 1061.
39. J. PEREZ and J. Y. CAVAILLE, *J. Non-Cryst. Solids*, 172–4 (1994) 1028.
40. J. PEREZ, "Physique et mécanique des polymères amorphes" (Lavoisier, Paris, 1992).
41. J. Y. CAVAILLE, J. PEREZ and G. P. JOHARI, *Phys. Rev. B* **39** (1989) 2411.
42. J. PEREZ, J. Y. CAVAILLE, S. ETIENNE and F. FOUQUET, *J. Phys.* **41** (1980) C8-850.
43. J. PEREZ, in "International Summer School on Mechanical Spectroscopy", Cracow, Poland, Proc., ed. I. Magalas, Chapman & Hall, forthcoming.
44. G. VIGIER and J. TATIBOUET, *Polymer*, **34** (1993) 4257.
45. O. A. HASSAN and M. C. BOYCE, *Polym. Eng. Sci.* **35** (1995) 331.
46. P. B. BOWDEN and S. RAHA, *Philos. Mag.* **29** (1974) 149.
47. V. A. BERSHTEIN, V. M. YEGOROV, L. G. RAZGULYAYEVA and V. A. STEPANOV, *Polym. Sci.* USSR **20** (1978) 2560.
48. E. J. KRAMER, *J. Polym. Sci. Polym. Phys.* **13** (1975) 509.
49. W. M. PREST and F. J. ROBERTS, *Ann. N.Y. Acad. Sci.* **371** (1981) 67.
50. T. M. KUNG and J. C. M. LI, *J. Polym. Sci. Polym. Chem.* **24** (1986) 2433.
51. S. S. STERNSTEIN and F. A. MYERS, *J. Macrom. Sci. Phys.* **B8** (1973) 539.

Received 22 December 1994
and accepted 13 February 1996